Carbohydrate Polymers 104 (2014) 8–16

Contents lists available at ScienceDirect

Carbohydrate Polymers

journal homepage: www.elsevier.com/locate/carbpol

Enhanced adsorption of methyl violet and congo red by using semi and full IPN of polymethacrylic acid and chitosan

Jayabrata Maity, Samit Kumar Ray*

Department of Polymer Science and Technology, University of Calcutta, 92, A.P.C. Road, Kolkata 700009, India

ARTICLE INFO

Article history:
Received 20 November 2013
Received in revised form
28 December 2013
Accepted 30 December 2013
Available online 7 January 2014

Keywords:
IPN
Chitosan
Methacrylic acid
Characterization
Dye removal

ABSTRACT

Semi and full interpenetrating polymer network (IPN) type hydrogels were prepared by free radical in situ polymerization of methacrylic acid in presence of chitosan using N,N′-methylene-bis-acrylamide (MBA) and glutaraldehyde (for full IPN) as crosslinker. Several semi and full IPN type hydrogels were prepared by varying initiator and crosslinker concentration and also monomer to chitosan mass ratio. These hydrogels were characterized and used for removal of methyl violet and congo red dye from water. Isotherms and kinetics of dye adsorption were also evaluated.

1. Introduction

Hydrogel is a three dimensional polymer network containing various hydrophilic functional groups. Hydrogels are prepared by crosslinking natural or synthetic polymers. Natural polymers are biocompatible and biodegradable but hydrogels based on natural polymers are of poor mechanical strength while most of the hydrogels based on synthetic polymer are strong but not biodegradable. Thus, in recent times hydrogels are being prepared by combining both synthetic and natural polymers (Mandal & Ray, 2013). Interpenetrating network type hydrogel (IPN) is formed by interpenetration of two polymers and crosslinking either one of the polymers to form semi-IPN or both polymers to form full IPN type network (Sperling, 1981). Accordingly, a synthetic monomer may be polymerized in presence of a natural polymer followed by crosslinking of one polymer to form semi-IPN or both of the polymers to form full IPN hydrogels. In recent times semi and full IPN type hydrogels based on synthetic polymers such as acrylics and chitosan type natural polymer have been reported by many researchers (Crini & Badot, 2008). Chitosan, (1-4)-2-amino-2-deoxy-β-D-glucan, the cationic deacetylated derivative of chitin, is a well affirmed biopolymer owing to biocompatibility, biodegradability and absence of toxicity (Muzzarelli, 2012; Muzzarelli et al., 2012). Presence of reactive hydroxyl (—OH) groups at C-3, C-6 and amino ($—NH_2$) groups at C-2 position in chitosan makes it a potential adsorbent for dyes (Crini & Badot, 2008). Further, it is abundant in nature and thus low in cost. Wang et al. grafted acrylic acid onto chitosan filled with attapulgite for adsorption of methylene blue dye from water (Wang, Zheng, & Wang, 2009). Lee et al. (1999) synthesized semi IPN hydrogels of acrylic acid and MBA in presence of chitosan. Wang et al. reported chitosan grafted acrylic acid/attapulgite composite gel for fast removal of methylene blue from water (Wang, Zhang, & Wang, 2011). Chen, Liu, Jin, and Chen (2005) developed a novel semi-IPN of chitosan and polymethacrylic acid using formaldehyde as a crosslinker. The hydrogel showed high swelling with excellent pH sensitivity in the range of pH 1.40–4.50. Khan, Othman, Razak, and Akil (2013) modified chitosan by polymerization of methacrylic acid and MBA in its matrix.

It is evident from the above discussion that chitosan has been chemically modified for improving its adsorption properties. The synthetic hydrogels based on polymethacrylic acid have also been widely used as adsorbents for metal ions and dyes (Panic, Madzarevic, Husovic, & Velickovic, 2013). The objective of the present work was to modify a conventional and widely used synthetic hydrogel like crosslinked polymethacrylic acid (PMAA) with an easily available natural polymer such as chitosan. Thus, in the present work semi and full IPN of polymethacrylic acid and chitosan were synthesized by incorporating varied concentrations of chitosan in the crosslinked PMAA gel. The resulting hydrogels containing numerous hydrophilic functional groups would be very effective for adsorption of polar organic molecules such as synthetic dyes over a wide range of pH from water. Among the various

* Corresponding author. Tel.: +91 33 23508386; fax: +91 33 23508386.
E-mail address: samitcu2@yahoo.co.in (S.K. Ray).

0144-8617/$ – see front matter © 2014 Elsevier Ltd. All rights reserved.
http://dx.doi.org/10.1016/j.carbpol.2013.12.086

industrial dyes, congo red and methyl violet are extensively used for coloring various textile and plastics materials (Li, Xu, Wang, Chen, & Feng, 2009). These aromatic organic compounds are not biodegradable and highly soluble in water. Removal of these dyes of high tinctorial values from water by using a low cost bioadsorbent would resolve the environmental pollution caused by these organics. Thus, in the present work the semi and full IPN gel of polymethacrylic acid and chitosan were used for removal of these dyes from water.

2. Experimental

2.1. Materials

Chitosan (85% deacetylation), methacrylic acid, N,N′-methylenebisacrylamide (MBA), potassium peroxydisulfate and sodium meta bisulfite were obtained from Fluka, USA and used as obtained. Methyl violet and congo red dyes used in sorption studies were purchased from SRL Chemical, India.

2.2. Methods

2.2.1. Preparation of the hydrogels

The semi IPNs were synthesized by free radical polymerization in water in a three-necked reactor at 30 °C for 3 h using potassium persulfate and sodium metabisulfite as redox pair of initiators. The reactor was fitted with a stirrer, a thermometer pocket and a condenser. At first 1 mass% chitosan solutions was made in deionised water in a 250 ml glass beaker by gradual addition of required amount of chitosan and 2 mass% of acetic acid to obtain a viscous solution. The monomer methacrylic acid was then added to the three neck reactor placed on a constant temperature bath. Temperature was maintained at 30 °C and aqueous solution of initiators was added to the reactor followed by the addition of MBA (crosslinker). After polymerization the reaction mixture was cooled to ambient temperature. Hydrogel obtained was cut into small blocks and then immersed into double distilled water for 48 h to remove water soluble oligomer, uncrosslink polymer and unreacted monomers from the gel. The gel obtained was dried in a vacuum oven at 60 °C to a constant weight. The dried gel was then disintegrated in a blender. The full IPN hydrogels were prepared in a similar way but glutaraldehyde (GLU) was added to the reaction mixtures for crosslinking chitosan.

2.2.2. Characterization of the hydrogels

The amount of free carboxylic groups present in the hydrogel and its pH at point of zero charge (PZC) were determined by methods reported elsewhere (Mandal, Ray, & Bhattacharyya, 2012; Wang et al., 2008). Fourier Transform Infrared spectra (FTIR) of the hydrogels were recorded on a FTIR spectrometer (Perkin Elmer Spectrum2, Singapore), using KBr pellet made by mixing KBr with fine powder of the polymer gel samples. The wide angle X-ray diffraction profile of the gel samples were studied in a diffractometer (model: X'Pert PRO, made by PANalytical B.V., The Netherlands) using Ni-filtered Cu K_α radiation (λ = 1.542 Å) and a scanning rate of 0.005° (2θ)/s). Differential thermal analysis (DTA) and thermogravimetric analysis (TGA) of the polymer samples were carried out in a in a Perkin Elmer instrument in nitrogen atmosphere at the scanning rate of 10 °C/min in the temperature range of 25–600 °C.

2.2.3. Study of dye adsorption by the hydrogels

Low (2.5–40 mg/l) and high (200–500 mg/l) concentration ranges of methyl violet and congo red were prepared in distilled water. Approximately, 50 mg of hydrogel was taken in known volume of the dye solution with continuous stirring on a magnetic stirrer until equilibrium was reached. After equilibrium the dye solution was separated by decantation from the hydrogel. The concentrations of dye solutions before and after addition of hydrogel were determined by spectrophotometric measurement from a precalibrated curve of absorbance versus concentrations using UV-visible Spectrophotometer (Perkin Elmer lambda 2.5). The absorbance of the dye solutions was measured at wavelength of 584 cm^{-1} for methyl violet and 495.2 cm^{-1} for congo red dye. The amount of dye uptake (in mg) by unit mass (in g) of the hydrogel at equilibrium (q_e, mg/g) was calculated using the following Eq. (1)

$$q_e = \frac{(C_i V_0 - C_e V)}{m} \quad (1)$$

Here C_i and C_e are initial and equilibrium concentration of dye in water (mg/L), respectively, while V_0 and V is volume of the initial and equilibrium dye solution containing the hydrogel, respectively and m is mass (g) of the xerogel used for the experiment. Similarly, dye removal% (R) was obtained as

$$R = \frac{(C_i - C_e)}{C_i} \times 100 \quad (2)$$

2.2.4. Dye adsorption isotherms

The distribution of dye molecules between adsorbent and aqueous phase at equilibrium is obtained from adsorption isotherms. Dye adsorption data at equilibrium (q_e) for various initial feed dye concentrations (C_e) were fitted to the following two-parameter Langmuir and Freundlich (Eqs. (3) and (4), respectively), three-parameter Sip (Eq. (5)) and four parameter Fritz–Schlünder isotherm (Eq. (6)) models (Garcia et al., 2004)

$$q_e = \frac{q_{\max} k_L C_e}{1 + k_L C_e} \quad (3)$$

$$q_e = k_F C_e^{1/n} \quad (4)$$

$$q_e = \frac{k_S C_e^{\beta_S}}{1 + a_S C_e^{\beta_S}} \quad (5)$$

$$q_e = \frac{a_{FS} C_e^{\alpha}}{1 + b_{FS} C_e^{\beta}} \quad (6)$$

where $q_{\max}$ is the maximum monolayer adsorption, k_L, k_F and k_S are Langmuir, Freundlich and Sip constant and n, α, β_s, β, a_{FS}, b_{FS}, are parameters concerning the respective model.

2.2.5. Dye adsorption kinetics

The mechanism of dye adsorption was evaluated in terms of adsorption kinetics by measuring adsorption (q_t) at various time intervals (t) till equilibrium value is reached (q_e) for a fixed initial feed concentration of dye (C_i). In the present system dye adsorption data were not found to give good fitting to pseudo 1st order rate kinetics (not shown). However, like swelling data, dye adsorption data was also found to show close fitting to the following non linear Ho and McKay pseudo second order kinetic Eq. (7) (Vaghani, Patel, & Satish, 2012). For evaluating diffusion mechanism of dye adsorption, intra particle diffusion model (Eq. (8)) of Weber and Morris (Panic et al., 2013; Wang, Zheng, & Wang, 2009) was also used.

$$q_t = \frac{q_e^2 k_{2HM} t}{1 + k_{2HM} q_e t} \quad (7)$$

$$q_t = k_{ip} t^{1/2} + c \quad (8)$$

where k_{2HM} is rate constant for the adsorption following second order rate equation, k_{ip} is rate constant for intra particle diffusion; c is intercept which signifies boundary layer resistance.

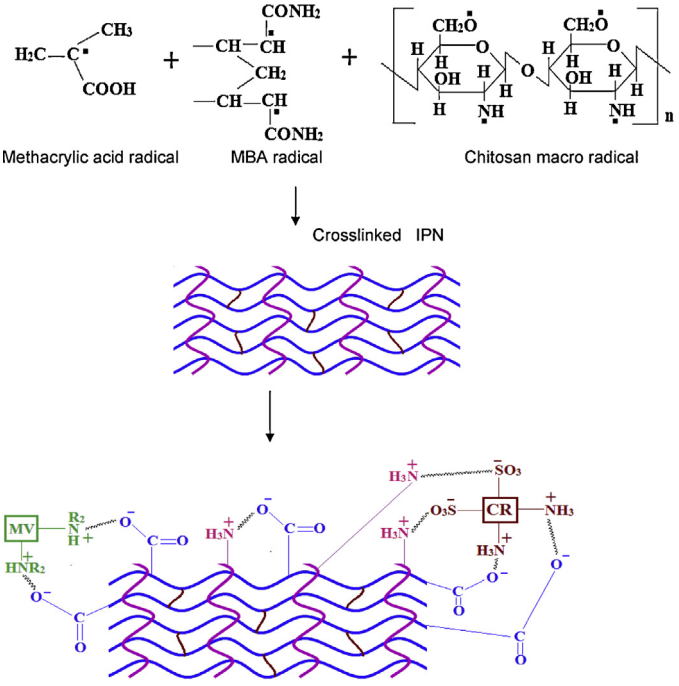

Scheme 1. Formation of IPN and its interaction with congo red (CR) and methyl violet (MV) dye.

2.2.6. Mass transfer coefficient (k_{mtc})

Mass transfer coefficient of the dye molecules at hydrogel–aqueous feed interface was determined by non linear fitting of dye adsorption data at various time intervals and at equilibrium to the following Eq. (9) (Dhodapkar, Rao, Pande, Nandy, & Devotta, 2007).

$$\ln\left(\frac{C_t}{C_i} - \frac{1}{(1+wk_L)}\right) = \ln\left(\frac{wk_L}{(1+wk_L)}\right) - \left(\frac{1+wk_L}{wk_L}\right) k_{mtc}At \quad (9)$$

Here A is surface area of the hydrogel sample of mass w, C_e is initial concentration of dye in feed while C_t is feed dye concentration at time t.

3. Results and discussion

3.1. Synthesis of IPN hydrogels

The polymerization reaction is initiated by reduction/oxidation (redox) reaction between potassium peroxydisulfate and sodium metabisulfite resulting in generation of free radicals. These radicals react with methacrylic acid and MBA to generate primary radicals. During 'propagation' reaction bifunctional MBA reacts with monofunctional methacrylic acid to form a network type radical. During polymerization reaction some of the amino (—NH_2) functional groups also initiate free radicals and these macro radicals of chitosan (Panic et al., 2013) also take part in the polymerization reaction to be part of the network gel. Some of the amino (—NH_2) groups of linear chitosan also form a polyeletrolyte type complex by reacting with carboxylic functional groups of methacrylic acid (Lee et al., 1999). The formation of the IPN and its interaction with dye is shown in Scheme 1.

3.2. Characterization of the hydrogels

The amount of free carboxylic acids in the gels was obtained by titrating with sodium hydroxide solution. The change of surface functionality of the hydrogels with solution pH was evaluated by determining pH at point of zero charge (PZC). The structure of the hydrogels, i.e., presence of various functional groups, its mutual electrostatic interactions, hydrogen bonding and crosslinking were evaluated by FTIR. Similarly, crystallinity of the hydrogels was characterized by XRD. Thermal stability and various transition temperatures of the hydrogels were studied by DTA-TGA. For these characterization the polymethacrylic acid gel synthesized with 1 wt% initiator and crosslinked with 1 wt% crosslinker (designated as PMAA), the semi IPN gel synthesized with 1 wt% chitosan, 1 wt% initiator and 1 wt% crosslinker (designated as CSMS) and the full IPN gel (designated as CSMF, same as CSMS but the chitosan moiety is crosslinked with 1 wt% glutaraldehyde) were considered.

3.2.1. Amount of carboxyl group in the hydrogel

The amount of free carboxyl groups present in CSMS and CSMF was 46.56% and 41.11%, respectively. The less number of free carboxylic groups in the full IPN (CSMF) may be ascribed to its tighter network because of crosslinking of the both of its constituent polymers.

3.2.2. pH at point of zero charge (PZC)

The change of state of ionization of the functional groups of the hydrogels with solution pH is evaluated in terms of its pH at point zero charge (PZC). The initial pH of a solution (pH_i) changes in presence of hydrogel or dye molecules. The difference between this final pH (pH_f) and initial pH (pH_i), i.e., $pH_i - pH_f$ is plotted against pH_i in Fig. 1a. The pH of the solution (pH_{PZC}) at which $pH_i - pH_f$ is zero is pH at PZC. Hydrogel will remain neutral at solution pH = pH_{PZC}, positively charged at solution pH < pH_{PZC} or negatively charged at solution pH > pH_{PZ}. From Fig. 1a it is observed that chitosan shows a pH_{PZC} of 9.98 as also reported elsewhere (Wang et al., 2008). It implies that chitosan will remain in protonated form even at very high pH (up to 9.98). It is also observed that pH_{PZC} values drastically decreases in semi and full IPN hydrogels and it was 6.56 and 7 for CSMS and CSMF, respectively. In fact, in presence of chitosan negative charge of polymethacrylic acid is reduced because of formation of poly ion complex (Lee et al., 1999). Thus, pH_{PZC} of IPN gel decreases. The full IPN shows slightly lower pH_{PZC} than semi-IPN which may be due to crosslinking of chitosan in the IPN hydrogels.

3.2.3. FTIR spectroscopy

Fig. 1b shows the FTIR spectra of chitosan, PMAA, CSMS and CSMF. For pure chitosan the broad band appearing at 3367 cm^{-1} corresponds to overlapping of —OH stretching vibration, symmetric N—H vibration and the intermolecular hydrogen bonding of its polysaccharide moiety (Dai, Yan, Yanga, & Cheng, 2010; Vaghani et al., 2012). The carbonyl stretching vibration (amide-I), N—H stretching vibration (amide-II) and the C—N stretching vibration (amide-III) of chitosan is indicated by its absorption at 1659, 1595 and 1321 cm^{-1}, respectively (Ahmed, Naik, & Sherigara, 2009). The absorption peaks at 2920 and 2879 cm^{-1} are due to C—H stretching vibration while peaks at 1379 and 1419 cm^{-1} are due to symmetrical deformation of methyl (CH_3) groups of chitosan (Ahmed et al., 2009). It also shows another broad band appearing at 1088 cm^{-1} due to its C—O stretching (Ahmed et al., 2009). In Fig. 1b PMAA hydrogel is observed to show a peak at 1716 cm^{-1} due to C=O stretching vibration of its carboxylic group and also two absorption peaks at 1265 and 1157 cm^{-1} corresponding to its carboxylic C—O stretching (Panic et al., 2013). Similarly, the absorption peak at 2961 cm^{-1} of PMAA is due to its CH_2 stretching (Garcia et al., 2004). No peak is observed for this polymer at 1656 cm^{-1} corresponding to C=C stretching of the vinyl unsaturated monomer (methacrylic acid) which also confirms polymerization of the acid (Rufino & Monteiro, 2000). Most of the peaks of chitosan and PMAA show a red shift in CSMS. Accordingly, the broad band appearing at 3367 cm^{-1} of chitosan is observed to shift to 3369 cm^{-1} in

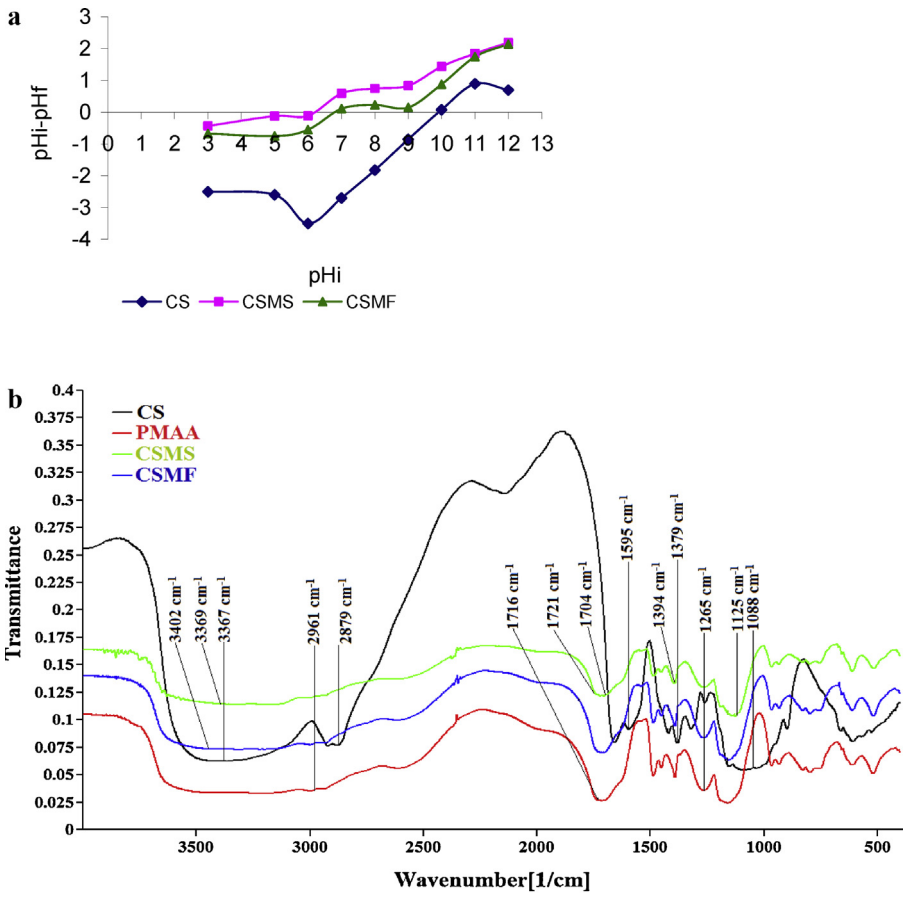

Fig. 1. (a) PZC of the polymer. (b) FTIR of the polymers.

CSMS. The 1088 cm^{-1} peak of chitosan due to its C—O stretching is shifted to 1125 cm^{-1} in CSMS. Similarly, its amide-I, II and amide- III absorption shifts to 1721, 1704 and 1394 cm^{-1}, respectively, in CSMS. The C—O stretching peaks of polymethacrylic acid also shifts to 1266 and 1192 cm^{-1} in CSMS. All of these shifting of absorption peaks signify different interactions such as hydrogen bonding between functional groups, intermolecular rearrangement and change in the configuration of the main chain of the two polymer moiety in the IPN (Liu, Zhou, Zhang, Yu, & Cao, 2013). Further, CSMS also shows absorption peaks at 1655 and 1394 cm^{-1} due to asymmetric and symmetric stretching of its caboxylate (COO^-) groups while the peak at 1543 cm^{-1} is due to its protonated amine ($NH3^+$) groups. It also confirms strong electrostatic interaction between carboxylic groups of PMAA and amine groups of chitosan in the semi IPN (Dai et al., 2010; Dash, Ferri, & Chiellini, 2012). As expected, the full IPN viz. CSMF is observed to show similar peaks like semi-IPN. In CSMF the hydroxyl groups of chitosan form chemical crosslink with glutaraldehyde. As a result it shows an absorption peak at 3402 cm^{-1} indicating its crosslinking (Dai et al., 2010).

3.2.4. XRD

XRD of the polymers are shown in Fig. 2a. Chitosan is a semi crystalline natural polymer. Accordingly, it shows a strong diffraction peak at around 20.1° associated with mixture of (0 0 1) and (1 0 0) and one weak diffraction peaks at 10.6° associated with mixture of its (0 0 1) and (1 0 0) planes (Dash et al., 2012; Qi, Xu, Jiang, Hu, & Zou, 2004; Lee et al., 1999). From Fig. 2a it is also observed that CSMS and CSMF shows similar diffraction pattern and in comparison to chitosan these IPNs show much reduction in peak intensity with displacement of 2θ to a lower value (ca. 16.4°) and new peak at 2θ of 31.4°. This may be attributed to the reduction in crystallinity as well as change in d spacing in the matrix of chitosan because of introduction of pendant polymethacrylic acid in the IPNs (Milosavljevíc, Milăsinovíc, Popovíc, Filipovíc, & Krůsí, 2011).

3.2.5. Thermal study

The thermal properties of the polymers were evaluated in terms of (i) DTA and (ii) TGA of the polymers as shown in Fig. 2b(i) and (ii), respectively. The DTA of the polymers are shown in Fig. 2b(i). The decomposition of chitosan occurs in the temperature range of 265–340 °C with exothermic DTA peaks at 270 and 325 °C due to thermal decomposition of its amino and N-acetyl residue (Nam, Park, Ihm, & Hudson, 2010). The CSMS and CSMF are observed to show endothermic peaks at 227 and 234 °C, respectively due to formation of —NH—CO— bond between protonated/non-protonated amine groups of chitosan and carboxylic/carboxylate groups of acid in the IPN above 200 °C (Lee et al., 1999). TGA and DTG of the polymers are shown in Fig. 2b(ii). It is observed that chitosan shows two regions of weight loss viz., around 10% in the temperature range of 90–260 °C due to loss of absorbed water and around 15–51% in the temperature region of 270–360 °C due to degradation of its main chain (Rajendran & Sivalingam, 2013). Chitosan also shows a residue of about 27% at 580 °C. The degradation of main chain of chitosan involves random splitting of its glycosidic bonds followed by further decomposition and formation of a series of lower fatty acids of C2, C3 and C6(Milosavljevíc et al., 2011). From the same figure PMAA is observed to show multiple degradation profile. Thus, it shows around 10% weight loss in the temperature region of 100–185 °C, 15–30% weight loss in the temperature range of 190–390 °C, 30–75% in the temperature range of 395–490 °C with a residue of around 15% at 580 °C. The first region of degradation corresponds to loss of bound water while the degradations at other

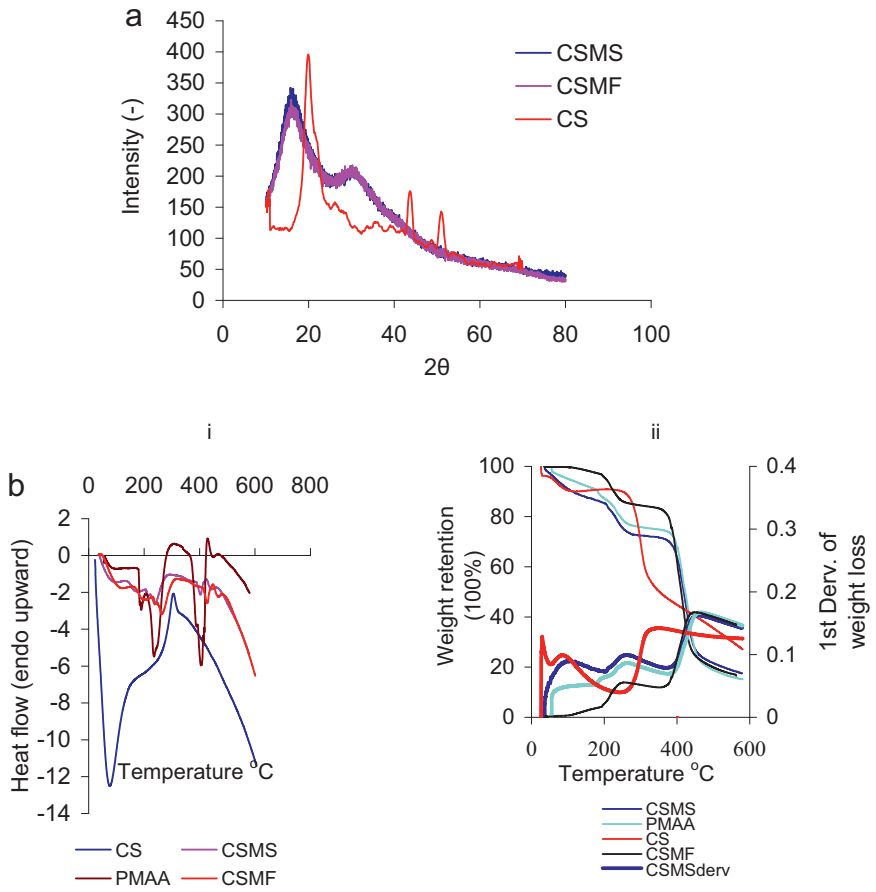

Fig. 2. (a) XRD of the polymer. (b): (i) DTA of the polymer, (ii) TGA and DTG of the polymers.

temperature regions may be ascribed to splitting of main chain and pendant carboxylic groups of PMAA (Milosavljevíc et al., 2011). The IPNs, i.e., CSMS and CSMF also show different degradation regions. Because of incorporation of chitosan and crosslinking of both acid and chitosan network, CSMF is observed to show much higher thermal resistance than PMAA (Mandal et al., 2012). The CSMS shows a degradation profile similar to CSMF but its thermal stability is observed to be marginally lower than PMAA. This may be because of poor interpenetration and crosslinking in CSMS where only the acid moiety is crosslinked with uncrosslinked chitosan in its matrix. Thus, loss of water is observed to occur at a lower temperature (95–130 °C) in the CSMS hydrogel.

3.3. Dye adsorption

3.3.1. Effect of solution pH on dye adsorption

The effect of solution pH on dye adsorption by the hydrogels at feed dye concentration of 2.5 mg/L is shown in Fig. 3a. Similar trends were also observed at other feed concentrations. For this pH responsive hydrogels dye adsorption increases with increase in solution pH. However, there is a sudden increase in dye adsorption as the solution pH increases from 4.2 to 7. Above this pH the dye adsorption by the hydrogels remains almost constant up to a pH of 9 and thereafter adsorption decreases marginally as the solution pH increases further from 9 to 10.2. The pK_a value of methacrylic acid is 4.65 while from Fig. 1a pH at point of zero charge (PZC) of chitosan, CSMS and CSMF are observed to be 9.98, 6.56 and 7, respectively. It indicates that the carboxylic groups of polymethacrylic acid and amine groups of chitosan will remain fully ionized in the pH range of 6.56–9.9. Accordingly, below solution pH of 6.56 (and 4.65 for PMAA), the carboxylic groups of the hydrogels are not in ionized form resulting in low dye adsorption. At solution pH of 10.2, the amine groups will deprotonate resulting in marginal decrease in dye adsorption for the hydrogels containing chitosan. Since the amount of chitosan is much less than PMAA, the change of adsorption above pH 9.9 was also marginal.

3.3.2. Effect of feed concentration on dye adsorption and removal%

The equilibrium adsorption (q_e, mg/g of gel) and removal% (*R*%) of low and high concentration ranges of methyl violet and congo red dye by PMAA, CSMS and CSMF hydrogels at pH of 7 are shown in Fig. 3b and c, respectively. It is observed from Fig. 3b and c that the hydrogels show high adsorption and removal% of the dyes. Thus, CSMS shows q_e of 1.7–7.14 mg/L and 1.62–6.12 mg/L and *R*% of 91–23 and 81.6–20.4 for congo red and methyl violet dye, respectively, in the low concentration range of 2.5–40 mg/L dye in feed. Similarly in the high concentration range of 200–500 mg/L, CSMS is observed to adsorb 146.5–229 mg/L of congo red and 142–220.6 mg/L of methyl violet at equilibrium. The high q_e and *R*% is caused by the strong electrostatic interactions among functional groups of the hydrogels and dye molecules (Mandal & Ray, 2013). Incorporation of chitosan in PMAA is also observed to cause significant increase in dye adsorption. Thus, for 2.5/200 mg/l congo red dye in feed removal% is observed to increases in the following order CSMS (91/98) > CSMF (89/95) > PMAA (87/92). Similar trend is observed for methyl violet. It is observed from Scheme 1 that congo red shows strong electrostatic interaction with the hydrogels through its two primary amine and sulfonic acid functional groups. The protonated amine and carboxylate functional groups of CSMS

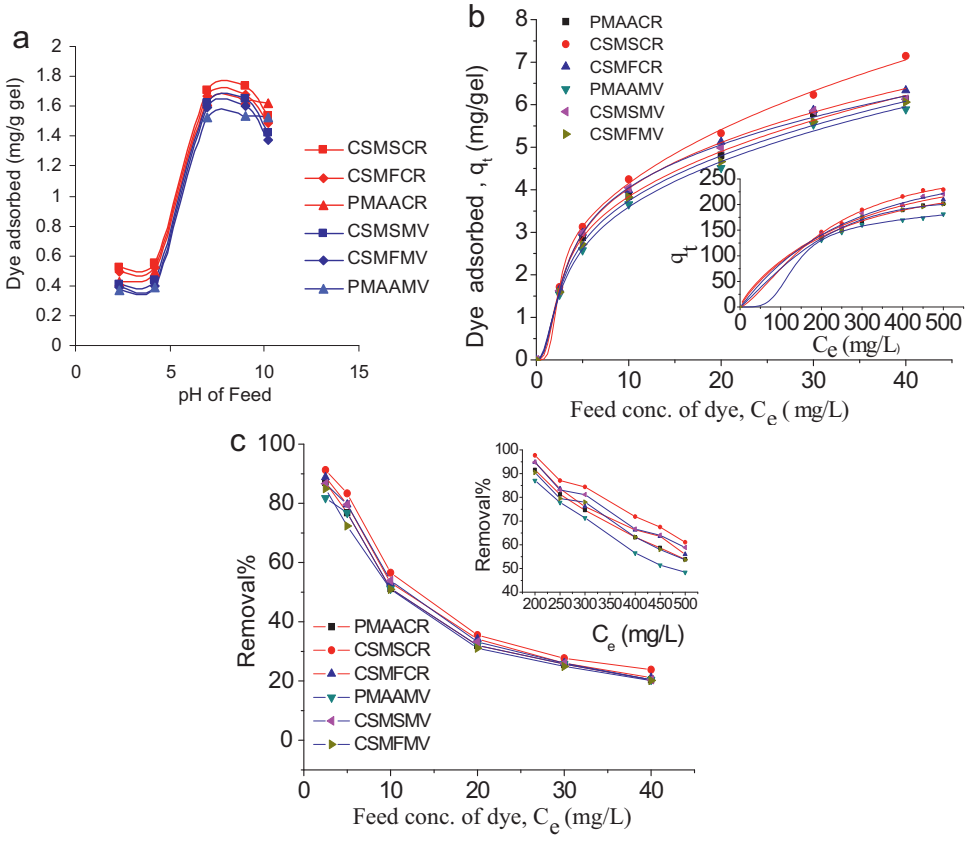

Fig. 3. (a) Effect of solution pH on dye adsorption, (b) effect of feed concentration on adsorption with Fritz–Schlünder isotherms and (c) effect of feed concentration on removal% of the dye.

hydrogel at experimental pH (7) show strong electrostatic interaction with amine and sulfonate functional groups of congo red dye. Thus, CSMS hydrogels shows the maximum dye adsorption with congo red dye. The methyl violet dye shows less adsorption in comparison to congo red since it contains only tertiary amine groups (Scheme 1). Thus, methyl violet-hydrogel electrostatic interaction will be less than congo red–hydrogel interaction (Al-Ghouti, Khraisheh, & Ahmad, 2005). Similarly, PMAA hydrogel shows less adsorption than the IPN gels since it contains only carboxylic functional groups in its structure. The marginally lower adsorption of CSMF than CSMS may be ascribed to the presence of slightly less number of free carboxylic groups in its structure. It is also observed that with increase in feed concentration of dye adsorption increases while removal% decreases. A given amount of hydrogel can adsorb a fixed amount of dye molecules. As the feed concentration increases, % of this fixed amount decreases with respect to increased feed concentration and hence dye removal% decreases at higher feed dye concentration (Bayramoglu, Altintas, & Arika, 2009).

3.3.3. Effect of contact time on dye adsorption

Effect of contact time on dye adsorption for a fixed concentration of dye, i.e., 2.5 mg/L (low concentration range) and 200 mg/L (high concentration range) is shown in Fig. 4a. It is observed that adsorption equilibrium (q_e) is attained at a much faster rate for low concentration. Thus, q_e is attained at around 900 min for high (200 mg/L) and 1400 min for low (2.5 mg/L) feed concentration. The dye molecules migrate from bulk aqueous feed to surface of the adsorbent by film diffusion and finally to the interior of the adsorbent gel by pore diffusion. Accordingly, the mass transfer resistance in the interface between bulk feed and surface of the hydrogel control dye adsorption. At higher feed dye concentration the mass transfer resistance of the boundary layer on gel surface is reduced with much reduction in equilibrium time (Bayramoglu et al., 2009).

3.3.4. Adsorption isotherms and kinetics

3.3.4.1. Fitting of dye adsorption data to adsorption isotherms. The dye adsorption data at varied feed concentrations were fitted to two-parameter Langmuir (Eq. (3)) and Freundlich (Eq. (4)), three-parameter Sip (Eq. (5)) and four-parameter Fritz–Schlünder (Eq. (6)) isotherms as also shown in Fig. 3b for Fritz–Schlünder model. Langmuir isotherm assumes that adsorption occurs at homogeneous sites of the hydrogels with little interaction among adsorbed solutes. The maximum adsorption (q_{max}) capacity of the hydogels is also obtained from this model. The dimensionless separation factor, R_L based on this model is

$$R_L = \frac{1}{1 + k_L C_i} \tag{10}$$

where K_L is Langmuir constant and C_i is initial dye concentration in feed. From Table 1 it is observed that the maximum monolayer adsorption (q_{max}) by the hydrogels as calculated from Langmuir model is close to the experimental maximum (equilibrium) adsorption values ($q_{maxexpt}$) in the low concentration ranges. Further, like $q_{maxexpt}$, calculated q_{max} and Langmuir constant K_L also increases in the following order CSMS > CSMF > PMAA for both low and high concentration range of the two dyes. Similarly, the values of R_L are observed to be in the range of 0.18–0.80 which also indicates favorable adsorption by Langmuir model. Freundlich isotherm relates to surface heterogeneity. From Table 1 it is also observed that the values of Freundlich parameter ($1/n$) are less than unity (0.39–0.49) which also indicates favorable adsorption by this isotherm. The dye adsorption data were also found to fit closely the

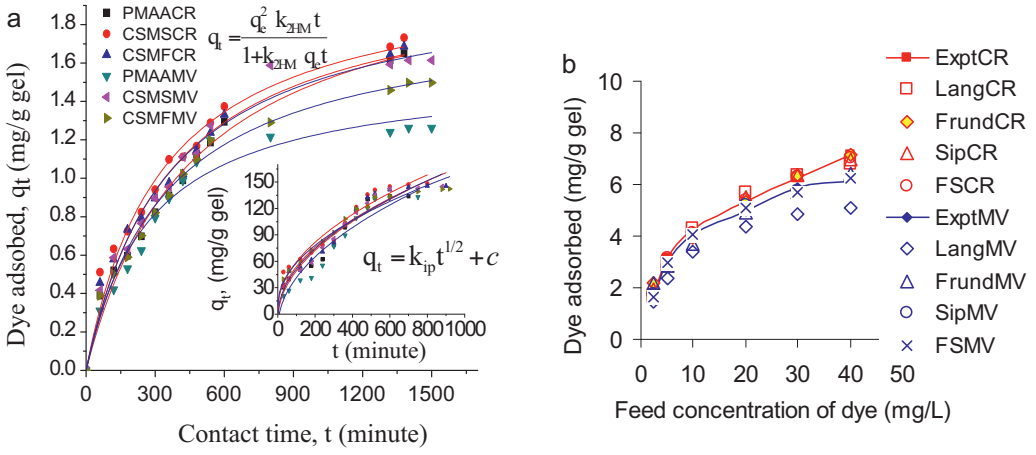

Fig. 4. (a) Effect of contact time on dye adsorption with pseudo 2nd order kinetics and inter particle diffusion (in inset). (b) Experimental and calculated adsorption data of CSMS.

Table 1
Parameter values of adsorption isotherms and adsorption kinetics models for low and high conc. of congo red (CR) and methyl violet (MV) dye.

Model	CR Low PMAA/CSMS/CSMF	MV low PMAA/CSMS/CSMF	CR High PMAA/CSMS/CSMF	MV High PMAA/CSMS/CSMF
Langmuir				
K_L (L/mg)	0.115/0.102/0.117	0.105/0.124/0.111	0.004/0.003/0.004	0.006/0.003/0.004
q_{max} (mg/L)	7.33/8.47/7.54	5.89/6.13/6.06	302/387/335	237/359/300
$q_{maxexpt}$ (mg/L))	6.13/7.14/6.33	5.89/6.12/6.06	202/229/210	182/221/201
R_L (–)	0.79–0.17	0.79–0.18	0.32–0.58	0.23–0.60
R^2	0.994//0.989/0.996	0.993/0.996/0.994	0.999/0.997/0.996	0.998/0.997/0.996
χ^2	0.032/0.068/0.0178	0.030/0.022/0.030	1.934/17.14/20.20	6.924/15.20/19.51
$F \times 10^{-2}$	18.75/10.94/36.09	17.92/28.66/19.08	481.3/68.52/50.38	112.6/70.06/47.68
Freundlich				
$1/n$	0.407/0.432/0.404	0.424/0.393/0.414	0.424/0.499/0.460	0.327/0.485/0.421
K_F (L/mg)	1.413/1.458/1.479	1.273/1.504/1.352	14.70/106712.47	23.81/11.01/14.99
R^2	0.987/0.989/0.985	0.989/0.980/0.988	0.998/0.995/0.995	0.996/0.996/0.993
χ^2	0.064/0.070/0.077	0.052/0.104/0.057	6.57/30.58/24.23	13.29/20.70/31.60
$F \times 10^{-2}$	9.29/10.60/8.33	10.43/5.96/10.00	141.54/38.40/42.10	58.69/51.47/29.44
Sip				
K_S (L/mg)	1.075/1.212/1.036	0.984/0.964/1.036	0.007/0.087/1.208	0.034/0.614/0.022
β_s	0.798/0.713/0.873	0.779/0.953/0.792	1.121/1.528/0.999	1.762/1.133/1.810
a_S	0.123/0.102/0.125	0.111/0.128/0.119	0.002/2.9E-04/0.004	2E-04/0.002/9.63E-5
R^2	0.994/0.992/0.997	0.994/0.994/0.994	0.999/0.998/0.995	0.998/0.997/0.996
χ^2	0.027/0.054/0.017	2.231/15.32/25.25	2.231/15.32/25.26	5.46/18.70/16.44
$F \times 10^{-2}$	14.54/9.25/25.04	15.24/15.67/15.27	278.13/51.11/26.87	95.14/37.98/37.74
FS[a]				
a_{FS}	1.75/1.72/1.99	1.66/2.14/1.75	2227/548/18037	49.8/640/10381
b_{FS}	7.16/31.52/5.1	3.33/5.91/4.27	1217/3790/6248	2.34E08/726/18197
α	0.342/0.382/0.315	0.34/0.29/0.34	-0.276/-0.09/-0.537	0.21/-0.09/-0.55
$-\beta$	2.9/4.7/2.3	2.08/2.3/2.33	1.15/1.49/1.29	4/1.1/1.62
R^2	0.997/0.998/0.999	0.996/0.997/0.998	0.999/0.996/0.994	0.998/0.995/0.996
χ^2	0.013/0.01/0.002	0.01/0.01/0.02	2.55/19.6/31.9	6.1/24.8/20.6
$F \times 10^{-2}$	22/34137	15.2/27.1/24.8	182/30/16	63/21/23
$k_{mtc} \times 10^5$	7.81/9.19/8.5	.26/7.74/7.71	9.63/11.7/11.2	9.11/10.5
Pseudo 2nd				
q_{ecal} (mg/g)	2.19/2.09/2.08	1.56/2.05/1.86	327/225/180	256/211/220
q_{eexpt} (mg/g)	1.65/1.73/1.68	1.26/1.61/1.49	134/148/145	133/145/142
$k_2 \times 10^3$ (g/mg min)	0.9/1.4/1.3	2.3/1.3/1.5	303/92/41	142/66/85
R^2	0.985/0.976/0.978	0.965/0.978/0.989	0.961/0.966/0.967	0.943/0.915/0.923
χ^2	0.032/0.0680.018	0.030/0.022/0.029	1.93/17/20	6.92/15.2/31.2
$F \times 10^{-2}$	18.75/10.94/36.09	17.92/28.66/19.08	48.30/68.52/50.30	112/70/30
Intraparticle				
k_p (mg/g min$^{1/2}$)	0.045/0.046/0.044	0.03/0.04/0.03	5.59/5.40/5.33	5.68/5.46/4.81
c	0.04/0.13/0.10	0.15/0.13/0.12	6.5/5.18/0.57	15/2/10
q_{ecal} (mg/g)	1.73/1.83/1.77	1.44/1.77/1.62	141/158/151	140/151/150
q_{eexpt} (mg/g)	1.65/1.73/1.68	1.26/1.61/1.49	134/148/145	133/145/142
R^2	0.978/0.969/0.977	0.923/0.941/0.956	0.946/0.955/0.941	0.965/0.966/0.965
χ^2	0.003/0.005/0.007	0.001/0.001/0.0008	3.78/29.69/13.72	5.57/4.54/11.54
$F \times 10^{-2}$	67.48/44.11/37.54	172.61/19.56/324.43	66.86/9.58/19.52	38.95/58.06/24.32

[a] FS – Fritz–Schlünder.

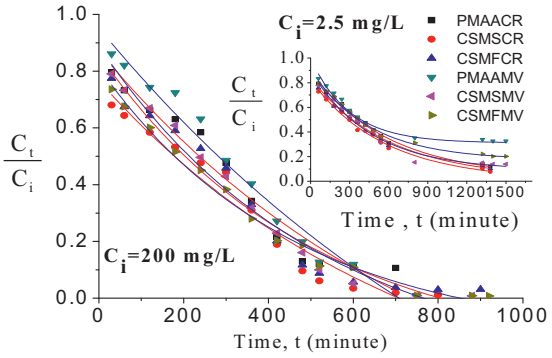

Fig. 5. Determination of mass transfer coefficient.

three parameter Sip and four-parameter Fritz–Schlünder model. Like Langmuir constant, Freundlich constant (K_F), Sip parameters (K_S, β, a_S), and Fritz–Schlünder constants (a_{FS}, b_{FS}, β, α) for these hydrogels also follow similar trend, i.e., CSMS > CSMF > PMAA. The statistical parameters, viz., R^2, χ^2 and F of all of these models are also shown in Table 1. The regression coefficient R^2 for these fittings is observed to be close to unity (0.989–0.999). These fittings also show low χ^2 and high F values. All of these confirms close fitting of experimental dye adsorption data to these models. Calculated dye adsorption data at various feed concentrations based on these four models are compared with experimental adsorption data for CSMS gel in Fig. 4b which also shows close fitting of the experimental dye adsorption data to these models.

3.3.5. Fitting of dye adsorption data to adsorption kinetics

3.3.5.1. Pseudo second order kinetics. From Fig. 4a it is evident that for high feed dye concentration (200 mg/l) the dye adsorption data (q_t) at various time intervals (t) shows close fittings to Ho and McKay pseudo second order rate equation (Eq. (7)). The calculated equilibrium adsorption value (q_{ecal}) based on pseudo second order kinetics is also very close to experimental equilibrium values (q_{eexpt}) for low concentration (not shown figure) as observed in Table 1. The statistical parameters also confirms close fitting in the low concentration ranges. It also indicates chemical adsorption involving electrostatic interaction between dye molecules and hydrogels as rate controlling step (Al-Ghouti et al., 2005).

3.3.5.2. Intra particle diffusion. The mechanism of diffusion of dye from water to hydrogel is explained by fitting dye adsorption data (q_t) at square root of various time interval ($t^{1/2}$) to intra particle diffusion model (Eq. (8)) as shown for high (200 mg/l) feed concentration in the inset of Fig. 4a. In fact, intra particles fittings show multi linearity which signifies various mechanisms for dye adsorption (Han, Wang, & Ma, 2011). In the present work non linear fitting was carried out by directly fitting q_t and t data in Eq. (8). From the values of statistical parameters, experimental (q_{eexpt}) and calculated q_e (q_{ecal}) (Table 1) it is evident that dye adsorption kinetics at 200 mg/l feed concentration show close fittings to intra particle diffusion for both low (2.5 mg/l, not shown in figure) and high (200 mg/l, shown in inset of Fig. 4b) feed concentration. The values of k_{ip} and c at 200 mg/l feed concentration is also observed to be higher than these values at lower feed concentration (2.5 mg/l) which also signifies decrease in external mass transfer and increase in boundary layer thickness of the hydrogels at higher feed concentration (Aksu, 2005).

3.4. Mass transfer coefficient (k_{mtc})

Mass transfer coefficient for dye adsorption was obtained by non linear fitting of dye adsorption data to Eq. (9) as shown in Fig. 5. The values of k_{mtc} for low and high feed concentration of the dyes are also shown in Table 1. The values of k_{mtc} are also observed to be higher for high concentration range (200 mg/l) for both of the dyes. It is also observed that congo red shows higher k_{mtc} than methyl violet for both high and low feed dye concentration.

4. Conclusion

Several semi and full interpenetrating network (IPN) type hydrogels were synthesized from chitosan and polymethacrylic acid by changing polymer: monomer mass ratios, initiator and crosslinker concentrations. The hydrogel synthesized with 1 wt% initiator, 1 wt% crosslinker and 4 wt% chitosan showed high adsorption and removal% of congo red and methyl violet dyes for both low and high concentration range from water. The adsorption of these dyes was higher at high feed dye concentration range. However, adsorption or removal% of congo red was higher than methyl violet for both concentration range. Adsorption data were also observed to fit well to pseudo second order kinetics in the low concentration range and several adsorption isotherms viz. Langmuir, Freundlich, Sip and FS models.

Acknowledgement

Authors are grateful to Council of Scientific and Industrial Research (CSIR, sanction no. 22(0547)/11/EMR-II), Govt. of India, for their financial support.

References

Ahmed, A. A., Naik, H. S. B., & Sherigara, B. S. (2009). Synthesis and characterization of chitosan-based pH-sensitive semi-interpenetrating network microspheres for controlled release of diclofenac sodium. *Carbohydrate Research*, *344*, 699–706.
Aksu, Z. (2005). Application of biosorption for the removal of organic pollutants: A review. *Process Biochemistry*, *40*, 997–1026.
Al-Ghouti, M., Khraisheh, M., & Ahmad, S. A. (2005). Thermodynamic behavior and the effect of temperature on the removal of dyes from aqueous solution using modified diatomite: A kinetic study. *Journal of Colloid Interface Science*, *287*, 6–13.
Bayramoglu, G., Altintas, B., & Arika, M. Y. (2009). Adsorption kinetics and thermodynamic parameters of cationic dyes from aqueous solutions by using a new strong cation-exchange resin. *Chemical Engineering Journal*, *152*, 339–346.
Chen, S., Liu, M., Jin, S., & Chen, Y. (2005). Synthesis and swelling properties of pH-sensitive hydrogels based on chitosan and poly(methacrylic acid) semi-interpenetrating polymer network. *Journal of Applied Polymer Science*, *98*, 1720–2172.
Crini, G., & Badot, P. M. (2008). Application of chitosan, a natural aminopolysaccharide, for dye removal from aqueous solutions by adsorption processes using batch studies: A review of recent literature. *Progress in Polymer Science*, *33*, 399–447.
Dai, J., Yan, H., Yanga, H., & Cheng, R. (2010). Simple method for preparation of chitosan/poly(acrylic acid) blending hydrogel beads and adsorption of copper(II) from aqueous solutions. *Chemical Engineering Journal*, *165*, 240–249.
Dash, M., Ferri, M., & Chiellini, F. (2012). Synthesis and characterization of semi-interpenetrating polymer network hydrogel based on chitosan and poly (methacryloylglycylglycine). *Materials Chemistry & Physics*, *135*, 1070–1076.
Dhodapkar, R., Rao, N. N., Pande, S. P., Nandy, T., & Devotta, S. (2007). Adsorption of cationic dyes on Jalshakti, super absorbent polymer and photocatalytic regeneration of the adsorbent. *Reactive and Functional Polymer*, *67*, 540–548.
Garcia, D., Escobar, J., Bada, N., Casquero, J., Hernáez, E., & Katime, I. (2004). Synthesis and characterization of poly(methacrylic acid) hydrogels for metoclopramide delivery. *European Polymer Journal*, *40*, 1637–1643.
Han, X., Wang, W., & Ma, X. (2011). Adsorption characteristics of methylene blue onto low cost biomass material lotus leaf. *Chemical Engineering Journal*, *171*, 1–8.
Khan, A., Othman, M., Razak, K., & Akil, H. (2013). Synthesis and physicochemical investigation of chitosan-PMAA-based dual-responsive hydrogels. *Journal of Polymer Research*, *20*, 273–281.
Lee, J. W., Kim, S. Y., Kim, S. S., Lee, Y. M., Lee, K. H. Y., & Kim, S. J. (1999). Synthesis and characteristics of interpenetrating polymer network hydrogel composed of chitosan and poly(acrylic acid). *Journal of Applied Polymer Science*, *73*, 113–120.
Liu, M., Zhou, Y., Zhang, Y., Yu, C., & Cao, S. (2013). Preparation and structural analysis of chitosan films with and without sorbitol. *Food Hydrocolloids*, *33*, 186–191.
Li, X., Xu, S., Wang, J., Chen, X., & Feng, S. (2009). Structure and characterization of amphoteric semi-IPN hydrogel based on cationic starch. *Carbohydrate Polymers*, *75*, 688–693.
Mandal, B., Ray, S. K., & Bhattacharyya, R. (2012). Synthesis of full and semi interpenetrating hydrogel from polyvinyl alcohol and poly (acrylic acid-co-hydroxyethyl

methacrylate) copolymer: Study of swelling behavior, network parameters, and dye uptake properties. *Journal of Applied Polymer Science*, *124*, 2250–2268.
Mandal, B., & Ray, S. K. (2013). Synthesis of interpenetrating network hydrogel from poly(acrylic acid-cohydroxyethyl methacrylate) and sodium alginate: Modeling and Kinetics study for removal of synthetic dyes from water. *Carbohydrate Polymers*, *98*, 257–269.
Milosavljevíc, N. B., Milăsinovíc, N. Z., Popovíc, I. G., Filipovíc, J. M., & Krŭsí, M. T. K. (2011). Preparation and characterization of pH-sensitive hydrogels based on chitosan, itaconic acid and methacrylic acid. *Polymer International*, *60*, 443–452.
Muzzarelli, R. A. A., Boudrant, J., Meyer, D., Manno, N., DeMarchis, M., & Paoletti, M. G. (2012). A tribute to Henri Braconnot, precursor of the carbohydrate polymers science, on the chitin bicentennial. *Carbohydrate Polymers*, *87*, 995–1012.
Muzzarelli, R. A. A. (2012). Nanochitins and nanochitosans, paving the way to eco-friendly and energy-saving exploitation of marine resources. *Polymer Science: A Comprehensive Reference*, *10*, 153–164.
Nam, Y. S., Park, W. H., Ihm, D., & Hudson, S. M. (2010). Effect of the degree of deacetylation on the thermal decomposition of chitin and chitosan nanofibers. *Carbohydrate Polymer*, *80*, 291–295.
Panic, V. V., Madzarevic, Z. P., Husovic, T. V., & Velickovic, S. J. (2013). Poly(methacrylic acid) based hydrogels as sorbents for removal of cationic dye basic yellow 28: Kinetics, equilibrium study and image analysis. *Chemical Engineering Journal*, *217*, 192–204.
Qi, L., Xu, Z., Jiang, X., Hu, C., & Zou, X. (2004). Preparation and antibacterial activity of chitosan nanoparticles. *Carbohydate Research*, *339*, 2693–2700.
Rajendran, K., & Sivalingam, T. (2013). Industrial method of cotton fabric finishing with chitosan–ZnO composite for anti-bacterial and thermal stability. *Industrial Crops and Products*, *47*, 160–167.
Rufino, E., & Monteiro, E. (2000). Characterization of lithium and sodium salts of poly (methacrylic acid) by FTIR and thermal analyses. *Polymer*, *41*, 4213–4222.
Sperling, L. H. (1981). *Interpenetrating polymer networks and related materials*. New York: Plenum.
Vaghani, S. S., Patel, M. M., & Satish, C. S. (2012). Synthesis and characterization of pH-sensitive hydrogel composed of carboxymethyl chitosan for colon targeted delivery of ornidazole. *Carbohydrate Research*, *347*, 76–82.
Wang, S. G., Sun, X. F., Liu, X. W., Gong, W. X., Gao, B. Y., & Bao, N. (2008). Chitosan hydrogel beads for fulvic acid adsorption: Behaviors and mechanisms. *Chemical Engineering Journal*, *142*, 239–247.
Wang, X., Zheng, Y., & Wang, A. (2009). Fast removal of copper ions from aqueous solution by chitosan-*g*-poly(acrylic acid)/attapulgite composites. *Journal of Hazardous Materials*, *168*, 970–977.
Wang, Li, Zhang, J., & Wang, A. (2011). Fast removal of methylene blue from aqueous solution by adsorption onto chitosan-*g*-poly (acrylic acid)/attapulgite composite. *Desalination*, *266*, 33–39.